



Research Article

Open Access, Volume 3

Genome-Wide Analysis of the Regulatory Network of Immune Infiltration-Related RAS and RBP Regulators in Metastatic Osteosarcoma

Nanyong Huang; Wei Zuo; Haoqun Yao*

Department of Orthopaedics, The First Affiliated Hospital of Nanchang University, Nanchang, Jiangxi 330006, China.

Abstract

Background: Osteosarcoma is a primary malignant bone tumor commonly found in children and young adults. The prognosis of patients with metastatic osteosarcoma is very poor. Different studies have shown that immune infiltration is associated with osteosarcoma metastasis. However, the cellular composition of immune infiltrates may vary slightly in osteosarcoma metastases. Recent studies have reported that abnormal alternative splicing regulation is related to the occurrence and development of cancer.

Materials and methods: In this study, we performed a genome-wide analysis of the regulatory network of immune infiltration-related regulated alternative splicing (RAS) and RNA-binding proteins (RBP) regulators in metastatic osteosarcoma. Analysis of the GSE87624 dataset identified 547 differentially regulated alternative splicing events (RASEs) and 219 differentially expressed RNA binding proteins (DERBPs) ($FC \geq 2$ or $FC \leq 0.5$, $FDR \leq 0.05$). The differential RASE genes were enriched in cell cycle, cell division, DNA repair, RNA splicing, and other pathways.

Results: Among the 219 DERBPs, 96 genes were up-regulated and 123 genes were down-regulated, and the down-regulated genes were mainly enriched in cell adhesion and extracellular matrix-related pathways. Finally, we obtained seven DERBPs and corresponding alternative splicing events associated with immune cells and explored the important role of the genome-wide RBP-RASE-immune microenvironment regulatory network in the proliferation and metastasis of osteosarcoma.

Conclusions: In this paper, we examined the immune infiltration-related RAS and RNA-binding proteins (RBP) regulation network in metastatic osteosarcoma on a genome-wide scale. That has important implications for developing effective treatment strategies and improving outcomes for osteosarcoma patients.

Keywords: Osteosarcoma; Genome-wide analysis; RNA-binding proteins; Alternative splicing; Immune infiltration.

Manuscript Information: Received: Feb 16, 2023; Accepted: Mar 13, 2023; Published: Mar 23, 2023

Correspondance: Haoqun Yao, Department of Orthopaedics, The First Affiliated Hospital of Nanchang University, 17 Yongwai Street, Nanchang 330006, Jiangxi, China. Email: yaohaoqun@qq.com

Citation: Huang N, Zuo W, Yao H. Genome-Wide Analysis of the Regulatory Network of Immune Infiltration-Related RAS and RBP Regulators in Metastatic Osteosarcoma. *J Oncology*. 2023; 3(1): 1079.

Copyright: © Yao H 2023. Content published in the journal follows creative common attribution license.

Introduction

Osteosarcoma (OS) is a malignant bone tumor commonly found in adolescents and young adults. It originates from primitive transformed cells, characterized by aggressive local growth and high metastases [1]. Although surgery combined with chemotherapy has greatly improved the prognosis of patients with osteosarcoma, the prognosis of metastatic or recurrent osteosarcoma remains suboptimal [2]. The prognosis is particularly poor in patients with metastatic osteosarcoma, whose 5-year survival rate is <30% [3,4]. In spite of several attempts over the past 20+ years using various chemotherapy regimens for osteosarcoma, survival rates have remained relatively stable, and there hasn't been an effective targeted treatment yet [5]. Given this, elucidating the molecular mechanisms of osteosarcoma occurrence, proliferation, metastasis, and recurrence are of great significance for developing effective therapeutic strategies and improving prognosis.

In recent years, growing interest has been shown in the pathophysiology and genetics of osteosarcoma, and various genomic studies employing Whole-Genome Sequencing (WGS) and/or Whole-Exome Sequencing (WES) have been published. Genetic heterogeneity, multiple chromosomal abnormalities, mutations, and the most up- and down-regulated genes can all be discovered by genome analysis [5,6]. Moreover, recent studies have suggested a connection between abnormal alternative splicing regulation and the occurrence or progression of cancer. However, there is no research on the RBP-AS regulatory network and its possible functions from the genome-wide level.

In this paper, we examined the immune infiltration-related RAS and RNA-binding proteins (RBP) regulation network in metastatic osteosarcoma on a genome-wide scale.

Materials and Methods

Data Collection

Download the published osteosarcoma transcriptome expression data GSE87624 from the GEO database, the data set cell samples are derived from patients Osteosarcoma tissue, transcriptome data obtained by high-throughput sequencing of 44 osteosarcoma patients and 3 control bone tissues. Based on the transcriptome data of primary and metastatic osteosarcomas, differential expression analysis of RBPs and RASEs was carried out, and the differentially expressed RBP genes and RASEs were identified. Co-expression analysis of differentially expressed RBP and RASE was performed to study the RBP-AS regulatory network in this disease. 44 osteosarcoma patient samples were determined to compare immune cell types and discover differentially expressed RBPs and alternative splicing events in 23 primary and 9 metastatic osteosarcoma tissues. RBP-related genes were collected in the relevant literature [7-10].

Retrieval and process of public data

The public sequence data files were obtained from the Sequence Read Archive (SRA). Using the NCBI SRA Tool fastq-dump, SRA Run files were converted to fastq format. Using a FASTX-Toolkit, the raw readings were cleaned of low-quality bases. The clean readings were then assessed using FastQC.

Reads alignment and differentially expressed gene (DEG) analysis

HISAT2 used clean reads to align to the mouse genome [11]. Ultimately, read count and fragments per kilobase of exon per million fragments mapped (FPKM) for each gene were evaluated using uniquely mapped reads. Using FPKM, the expression levels of the genes were assessed. We choose the DESeq2 software to gene differential expression analysis. In order to account for the variation in Library depth, DESeq2 will model the original reads and utilize the scaling factor. Then, in order to model the read count, DESeq2 estimates the gene dispersion and decreases these estimates to get estimates of dispersion that are more accurate. Finally, DESeq2 matches the model of a negative binomial distribution, and the Wald test or likelihood ratio test is used to evaluate the hypothesis. The differentially expressed between two or more samples can be examined using DESeq2. According to fold change (FC) and false discovery rate (FDR), the results of the study could well be utilized to assess if the gene is expressed differently. There are two critical factors: (1) FC: the ratio of the absolute change in expression; (2) FDR: The following were the significant differential expression requirements: $FDR \leq 0.05$ and $FC \geq 2$ or ≤ 0.5 .

Alternative splicing analysis

Using the ABL as a pipeline as previously described, the Alternative Splicing Events (ASEs) and regulated alternative splicing events (RASEs) between the samples were identified and measured [12,13]. In summary, splice junction readings were used by ABL to detect 10 different forms of ASEs. Using the alternatives reads and models reads of the samples as raw data, Fisher's exact test was chosen to establish statistical significance for sample pair comparison. We determined the RASE ratio, which is the changed ratio of alternatively spliced reads and constitutively spliced reads between comparable samples. The threshold for RASEs detection was established at the RASE ratio ≥ 0.2 and the p-value ≤ 0.05 . To assess the significance of the ratio alteration of AS events, the Student's t-test for repeated comparison was used. Non-intron retention (NIR) RASEs were defined as events that were significant at a P-value cutoff of 0.05.

Functional enrichment analysis

Using the KOBAS 2.0 server, Gene Ontology (GO) keywords and KEGG pathways were found to classify DEGs into functional categories [14]. The enrichment of each term was determined by using hypergeometric test and the Benjamini-Hochberg FDR controlling procedure. The study of functional enrichment of the sets of selected genes also included Reactome pathway profiling.

Immune cell infiltration analysis tool

For the analysis of immune cell infiltration, we used the IOBR package in the R package, which was published in *frontiers in immunology* on July 2, 2021 (IF=7.561). ESTIMATE, CIBERSORT, xCell, TIMER, IPS, MCPcounter, EPIC, and quantTiseq are 8 published methods for decoding tumor microenvironment (TME) contexture that are combined in IOBR. Additionally, 255 published signature genes set including the tertiary lymphoid structure, tumor microenvironment, m6A, microsatellite instability exosomes, and tumor metabolism were gathered by IOBR. Additionally, IOBR employs a variety of methods for data analysis, variables transformation, feature selection, and supports batch survival analysis and

even visualization of corresponding result.

Construction of PPI Network

PPI information of all RBP and RASE that were differentially expressed was downloaded after processing by STRING database. To create the PPI network, we used the Cytoscape software (correlation coefficient ≥ 0.6).

Other statistical analysis

Principal component analysis (PCA) was performed by R package *factoextra* to show the clustering of samples with the first two components. The next-generation sequencing data and genomic annotations were visualized in *house-script* (*sogen*) after normalizing the reads by TPM of each gene in the samples. The clustering based on Euclidean distance was performed by using the *heatmap* package in R. The Student's t-test was employed to compare the two groups.

Results

Analysis of gene expression profile of metastatic and primary osteosarcoma (OS)

Transcript data of primary osteosarcoma and metastatic osteosarcoma samples were obtained from the dataset GSE87624. A hierarchical clustering heatmap was used to show a correlation between metastatic and primary sample based on all expression genes' FPKM value (Figure 1A). To find the differentially expressed genes between primary and metastatic osteosarcoma, we used differential analysis with the R package *limma* ($FDR \leq 0.05$ and $FC \geq 2$ or ≤ 0.5). The volcano plot showed that 96 genes were up-regulated and 123 genes were down-regulated in metastatic osteosarcoma tissue compared with primary osteosarcoma (Figure 1B). PCA of all differentially expressed genes in primary and metastatic osteosarcoma was performed using the R software package *factoextra*, which clearly showed the results (Figure 1C). For gene function enrichment analysis, we applied the GO annotations of the genes in the R package as the background to map the genes to the background set and enriched them using KOBAS 2.0 server analysis. The results of the gene set enrichment were then obtained. The GO functional enrichment analysis showed that the up-regulated genes were primarily enriched in the development and cell differentiation-related pathway of multicellular organisms, and the down-regulated genes were mainly enriched in the cell adhesion and extracellular matrix-related pathways (Figure 1D,E).

In addition, the most recent KEGG Pathway gene annotation was obtained via the KEGG rest API. The same method was adopted to obtain KEGG functional enrichment analysis, which showed that up-regulated genes were primarily enriched in Lysosomal and Vascular smooth muscle contraction pathways, while down-regulated genes were mainly enriched in Mucin type O-glycan biosynthesis and Neuroactive ligand-receptor interaction pathways (Figure 1F,G).

Abnormal alternative splicing patterns in metastatic OS compared with primary OS

First, we used ABL to calculate the ratio of changes in alternately and constitutively spliced read between the sample, determined as the RASE ratio. RASE ratios ≥ 0.2 and p-values ≤ 0.05 were set as thresholds for the detection of RASEs, and significant

events with p-values ≤ 0.05 were considered non-intron-retaining regulated alternative splicing events (NIR RASEs). On this basis, we obtained all RASEs in metastatic and primary samples, as well as 547 NIR RASs that significantly differed between the two samples (Figure 2A,B). PCA of these NIR RASs was also performed, clearly distinguishing the two samples (Figure 1C). A hierarchical clustering heatmap of RAS was drawn based on splicing ratio, and differences between metastatic and primary osteosarcoma were clearly identified (Figure 1D). Finally, we used GO and KEGG functional enrichment analysis to enrich the genes corresponding to these 547 differential RASEs. GO functional enrichment analysis showed that these genes were mainly enriched in Cell cycle, Cell division, Protein transport, DNA repair, RNA splicing and other pathway (Figure 2E). The KEGG functional enrichment analysis indicated that it was mainly enriched in Autophagy, Base excision repair, Amino acid degradation, and Bacterial infection pathways (Figure 2F).

Dynamic changes of ASE associated with immune microenvironment regulation in OS

Based on the expression profiles of metastatic and primary samples, the R software package *IOBR* package was used to select the CIBERSORT calculation method and obtain immune infiltrating cell scores for the two groups of samples. Boxplots were used to show the differences in immune cell types between the two samples (Figure 3A). Significant increases in T follicular helper cell, activated memory CD4 T cell, and plasma cell were seen in metastatic osteosarcoma (Figure 3D). This result was slightly different from the recent results reported by Yang *et al.* who showed increased numbers of natural killer cells CD56, B cells naive, macrophages M1, and neutrophils in non-metastatic osteosarcoma tissue, while in non-metastatic osteosarcoma tissue macrophages M2 levels were higher in metastatic tissues [15]. However, this is consistent with the findings on osteosarcoma lung metastasis reported by Chen *et al.* [16]. who argued that plasma cells, activated memory CD4 T cells, T cells CD8, and Tregs were the key determinants of osteosarcoma tissue metastasis. PCA based on fractions of different immune cells of all expressed genes in the two groups of samples could also distinguish between the two (Figure 3B). In addition, the proportion of immune cells in metastatic compared to primary osteosarcoma showed a decreasing trend (Figure 3C). The co-expression of RAS and 20 immune cell types was analyzed, and the pairs with a correlation coefficient ≥ 0.6 were selected. The regulated alternative splicing genes (RASG) - PDE4DIP, BSCL2, UBE2I, PLD3, CBWD5, and KIAA1841 were found to be significantly associated with plasma cells. Naive B cells were significantly associated with BSCL2, DPY19L3, BBC3, and KIAA1814. T cells CD8 were significantly associated with ZNF410, DPY19L3, and BBC3. Both activated CD4 memory T cells and Tregs were significantly associated with CCNL1. T follicular helper cells were significantly associated with BSCL2 and DPY19L3 (Figure 3E). Finally, we found the fractions of different immune cells estimated by CIBERSORT in each sample. There were a large number of plasma cells, T cells CD4, and T cells CD8 in the metastatic osteosarcoma tissue on the left side of the figure (Figure 3F). In conclusion, we found that after the metastasis of osteosarcoma, the immune infiltrating cells were mainly divided into plasma cell, CD8 T cell, activated memory CD4 T cell and Tregs.

Differential RBP regulates alternative splicing events related to immune cells.

In order to obtain differentially expressed RNA-binding protein (DERBP) genes between metastatic and primary samples, we used the Venn diagram to intersect 219 DEGs with 2494 RBP genes (obtained from ENCORI database) and finally obtained the top7 DERBP genes (Figure 4A). Next, we compared the expression of these DERBP genes in metastatic and primary osteosarcoma by boxplot, finding that the expressions of CRYAB, FBN1, TRIM61, and RBM20 were significantly down-regulated in metastatic osteosarcoma tissues, while the expressions of FAM184B and WIPF3 were significantly up-regulated in metastatic osteosarcoma tissues (Figure 4B). In order to understand the relationship between DERBP, RASE, RASG, and RAS-related immune cells, we used a Network diagram, which revealed that five DERBPs (WIPF3, FAM184B, RBM20, TRIM61, CRYAB) were associated with RAS-related immune cells (Figure 4C). The boxplot of the RAS splicing ratio associated with immune cells showed that the splicing ratio of ZNF410 was significantly down-regulated in metastatic osteosarcoma tissues, and the splicing ratio of BSCL2, CBWD5, and KIAA1841 was significantly up-regulated in metastatic cancer tissues (Figure 4D). Among them, the alternative splicing event ZNF410 regulated by CYRAB has negatively correlated with T cells CD4 memory activated, and the alternative splicing event BSCL2 regulated by WIPF3 was positively correlated with plasma cells. Finally, we found that the read distribution of NIR 17199 BSCL2 and NIR 31762 ZNF410 alternative splicing events were related to immune cells (Figure 4E-F). In conclusion, we speculate that CRYAB and WIPF3 may af-

fect the composition of immune cells by regulating gene alternative splicing, thereby promoting the metastasis of osteosarcoma tissue.

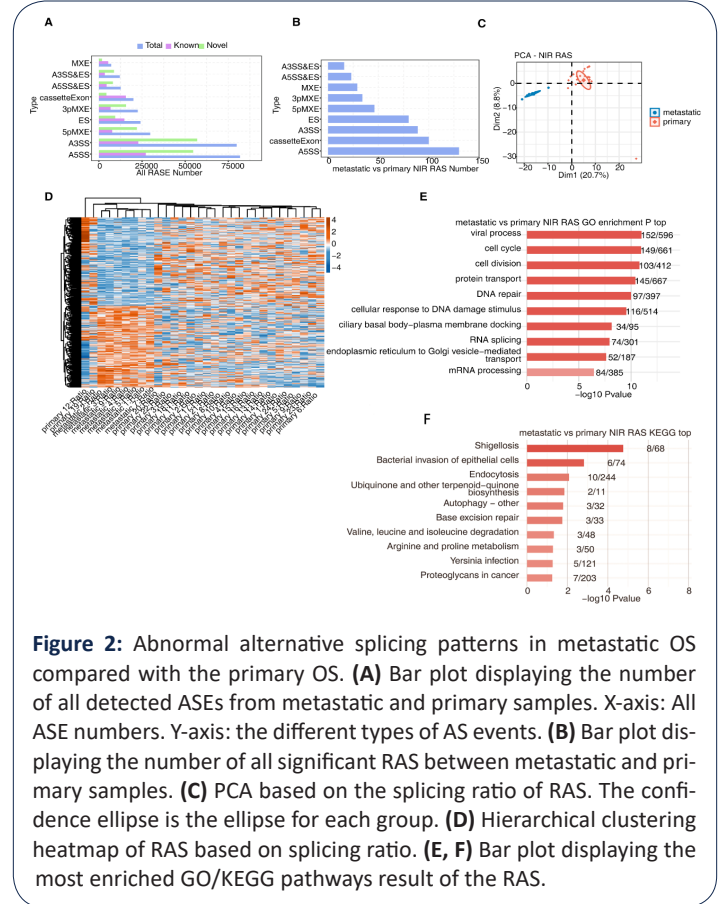
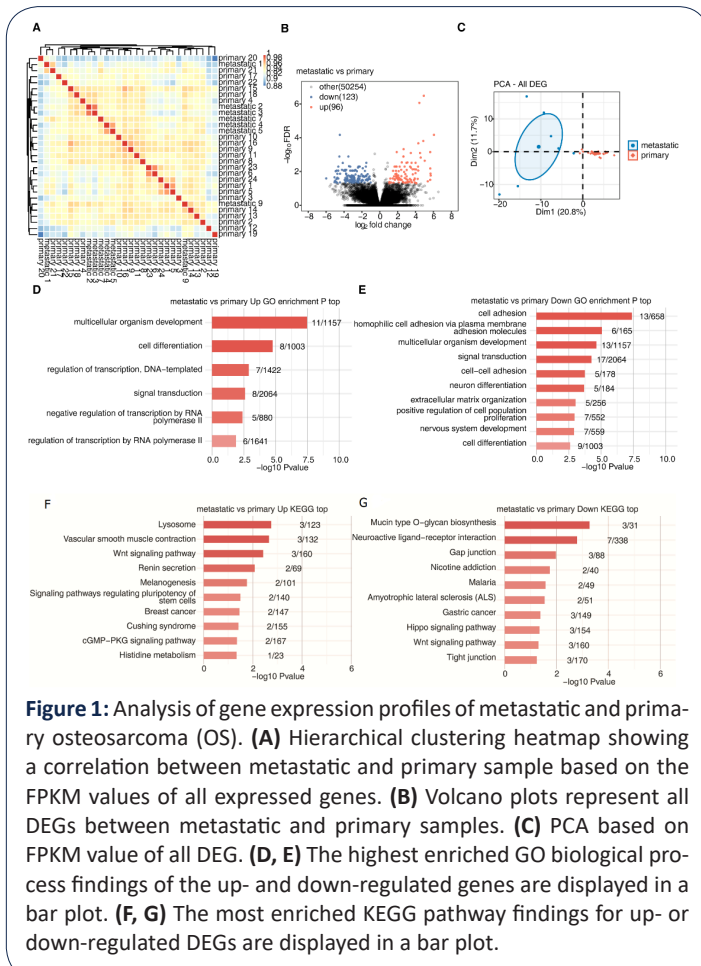


Figure 2: Abnormal alternative splicing patterns in metastatic OS compared with the primary OS. **(A)** Bar plot displaying the number of all detected ASEs from metastatic and primary samples. X-axis: All ASE numbers. Y-axis: The different types of AS events. **(B)** Bar plot displaying the number of all significant RAS between metastatic and primary samples. **(C)** PCA based on the splicing ratio of RAS. The confidence ellipse is the ellipse for each group. **(D)** Hierarchical clustering heatmap of RAS based on splicing ratio. **(E, F)** Bar plot displaying the most enriched GO/KEGG pathways result of the RAS.

RBPs are protein that bind to RNAs through globular RNA-Binding Domains (RBDs), thereby altering the function or fates of the bound RNAs [17]. RBPs can recognize special RNA-binding domains to interact with RNA and participate in various post-transcriptional regulatory processes, such as RNA splicing, transportation, polyadenylation, intracellular localization, translation, and degradation [18]. RNA alternative splicing refers to the process of transcribed precursor mRNA by removing introns and retaining exons to form mature mRNA, which is a vital step in regulating post-transcriptional gene expression. As regulation has an affect on more over 90% of human genes, including genes related with tumors [19].

The fundamental mechanism of RBP expression and its possible roles are revealed, which helps in the discovery of novel therapeutic targets as well as innovative methods or ideas. DDX24, DDX21, and IGF2BP2 in RBPs are associated with the prognosis of osteosarcoma, and WARS may have an important role in the immune infiltration of osteosarcoma [20]. PUM2 expression was shown to be low in osteosarcoma patients, and *Hu et al.* found that increasing PUM2 expression might inhibit osteosarcoma cells from migrating and progressing [21]. Moreover, IGF2BP1 expression is up-regulated in osteosarcoma tissues and seems closely related to the poor prognosis of patients with osteosarcoma [22]. *Pan et al.* found that the expression of HuR is significantly increased in osteosarcoma tissues, and inhibition of HuR could inhibit the viability, EMT, and promote apoptosis of osteosarcoma cells [23]. A recent study suggested PTBP1 as an oncogene in va-

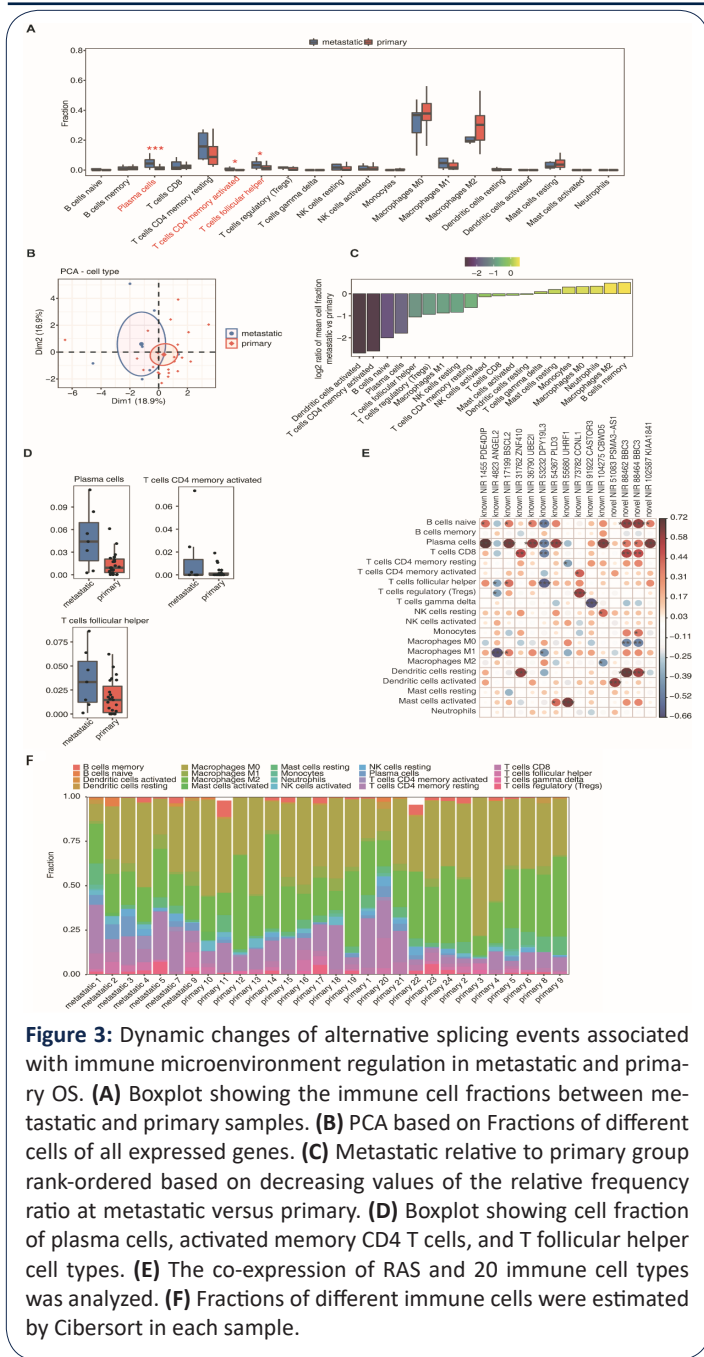


Figure 3: Dynamic changes of alternative splicing events associated with immune microenvironment regulation in metastatic and primary OS. (A) Boxplot showing the immune cell fractions between metastatic and primary samples. (B) PCA based on Fractions of different cells of all expressed genes. (C) Metastatic relative to primary group rank-ordered based on decreasing values of the relative frequency ratio at metastatic versus primary. (D) Boxplot showing cell fraction of plasma cells, activated memory CD4 T cells, and T follicular helper cell types. (E) The co-expression of RAS and 20 immune cell types was analyzed. (F) Fractions of different immune cells were estimated by Cibersort in each sample.

rious cancers [24]. PTBP1 expression was vastly higher in chemotherapy-resistant than chemotherapy-sensitive osteosarcoma tissues, while PTBP1 knockdown enhanced the anti-proliferative and apoptosis-inducing effects of cisplatin in MG-63 and U2OS. Transcriptome sequencing showed that knockdown of PTBP1 could up-regulate the expression of copper transporter SLC31A1, and immunoprecipitation experiments showed that PTBP1 influences the expression level of SLC31A1 by affecting the stability of the SLC31A1 mRNA. According to *Niu et al.* [25], osteosarcoma tissues have higher levels of MSI1 expression than adjacent tissues, and MSI1 knockdown in osteosarcoma cells can inhibit cancer cell proliferation and tumor formation. MSI1 was able to bind to the 3'UTR sections of the p21 and p27 mRNAs, according to luciferase experiments. RBM10 has long been regarded as a tumor suppressor due to its ability to control the MDM2-p53 negative feedback loop, inhibits the expression of apoptosis proteins like Bcl-2 and Bax, and promotes the expression of caspase-3 and the produc-

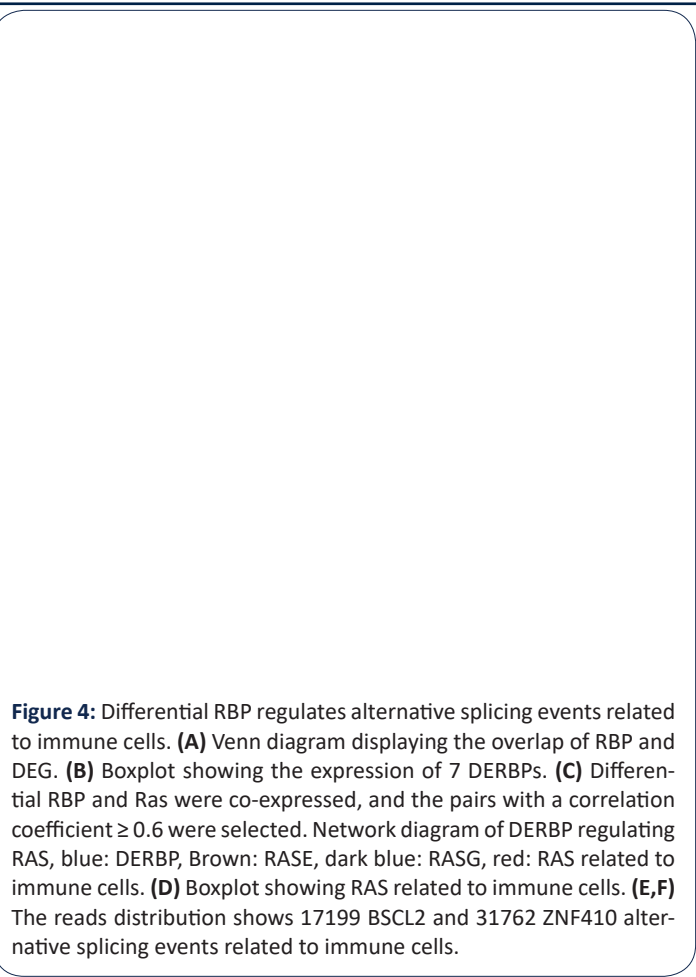


Figure 4: Differential RBP regulates alternative splicing events related to immune cells. (A) Venn diagram displaying the overlap of RBP and DEG. (B) Boxplot showing the expression of 7 DERBPs. (C) Differential RBP and Ras were co-expressed, and the pairs with a correlation coefficient ≥ 0.6 were selected. Network diagram of DERBP regulating RAS, blue: DERBP, Brown: RASE, dark blue: RASG, red: RAS related to immune cells. (D) Boxplot showing RAS related to immune cells. (E,F) The reads distribution shows 17199 BSLC2 and 31762 ZNF410 alternative splicing events related to immune cells.

tion of TNF- α , thereby inducing osteosarcoma cell apoptosis and inhibits cell proliferation via Notch signaling and the rap1a/Akt/CREB pathway [26].

Aberrant alternative splicing is prevalent in osteosarcoma, and its regulation has an important role in the development of osteosarcoma. There are previous reports of aberrant alternative splicing regulation of some genes. For example, loss or frequent down-regulation of cellular expression of leptin receptor overlapping transcripts may be associated with tumor formation. *Rothzerg et al.*, [27] analyzed the AS and transcriptional events between tumor and normal samples and discovered that up-regulating the expression of IL-6 and TNF- α via overlapping transcription of leptin receptors may influence the occurrence and metastasis of OS. SRSF3, a member of the Serine/Arginine-Rich (SR) protein family, regulates gene expression of FoxM1, PLK1, and CDC25B as well as protein translation, pri-miRNA processing, polymerization, polyadenylation, and regulates RNA alternative splicing in U2OS osteosarcoma cells [28]. In human osteosarcoma U2OS cells, *Ajiro et al.* [29] presented a genomic map of SRSF3-regulated RSE and gene expression, whose major transcripts contain highly conserved RNA motifs, revealing that splicing events were mainly associated with cell proliferation or cell cycle. Osteosarcoma (OS) is a representative tumor associated with the Human Telomerase Enzyme Reverse Transcriptase (hTERT) gene, whose Telomere Maintenance Mechanism (TMM) includes two forms of Telomerase Activity (TA) and alternative lengthening telomere (ALT). *Hitomi et al.* showed that the control of hTERT expression includes both transcriptional and post-transcriptional

processes, both of which contribute to the occurrence of TMM (TA and ALT) in OS and may provide insight into the prognosis of patients [30]. In conclusion, both RBPs and AS link the exons of pre-mRNA in different arrangements, making gene expression patterns more complex, transcriptionally efficient, and promoting protein diversity. This eventually results in structurally and functionally distinct mRNA and protein variants and has an important role in disease.

RASE associated with immune infiltration in OS

With changes in the host immune system, the functional components of tumor-infiltrating immune cells (TIICs) undergo minor changes, and TIICs have been reported to be associated with clinical outcomes in cancer patients [31]. Osteosarcoma is an immune-sensitive type of tumor, mainly infiltrated by heterogeneous immune cells such as neutrophils, dendritic cells, monocytes, mast cells, and macrophages [32-34]. Numerous studies have reported that TIIC subsets such as NK cells, memory T cells, and M1 macrophages are typically associated with good prognosis in osteosarcoma, whereas M2 macrophages and Treg cells are associated with terrible prognosis in osteosarcoma [35-37]. Additionally, CD4+ memory T cells, CD8+ T cells, NK cells, M1 macrophages, Treg cells, and plasma cells were identified in metastatic tissues as key determinants of osteosarcoma metastasis [38,39], which is consistent with our results. *Chen et al.* found that patrolling mononuclear cells (PMOs) inhibited lung metastasis of osteosarcoma while T follicular helper cell, monocytes, and resting mast cells were associated with favorable chemotherapy outcomes for osteosarcoma [16]. In the complex tumor ecology, in addition to immune cells, there are stromal cell subsets that can drive malignant tumor progressions, such as endothelial cells, fibroblasts, reactive astrocytes, and microglia. *Peng et al.*, [40] explored the potential mechanism through which the predictive splicing factor affects the overall survival of glioblastoma (GBM) patients by regulating RASE, and they also found an association between AS and immune cell infiltration types in tumor tissues of different subtypes of GBM, establishing that the enrichment of many immune-related pathways may be caused by differences in the recruitment or differentiation of various immune cells in malignancies. RAS is closely related to the regulation of the immune microenvironment during the occurrence of tumors. Therefore, we studied the correlation between immune cell types and RASE in osteosarcoma metastasis at the genome-wide level and analyzed their possible functions.

RASG associated with RBPs in tumors

Lipid droplet morphology is thought to be involved by the endoplasmic reticulum protein, which is encoded by the gene of BSCL2, and BSCL2 has been linked to both overall survival and progression-free survival in high-grade ovarian serous carcinoma (HGOSC) [41]. *Ali et al.* [42] analyzed ovarian cancer data from TCGA and showed that in univariate and multivariate analysis, the expression profile of the gene BSCL2 had a statistically significant correlation with the survival rate of ovarian cancer patients. However, as the gene has been studied to a lesser extent in osteosarcoma, the specific mechanism remains unknown. A transcription factor (TF) called ZNF410, also referred to as APA-1, regulates the expression of genes involved in matrix remodeling during the senescence of fibroblasts [43]. The research on ZNF410 is lacking,

yet, the latest cancer research reported the association of abnormal expression of this gene in breast cancer with tumor stage and different subtypes [44]. CBWD5, also known as CBWD3, is currently only reported to have copy number variation in CBWD5 in small cell lung cancer [45].

The blank of RBM10/20 and WIFE3 in osteosarcoma research

The expression of RBM10 can induce the apoptosis of osteosarcoma and inhibit the proliferation of primary chondrocytes by reducing the production of Bcl-2, increasing the production of caspase-3 and the expression TNF- α . However, over-expression of Bcl-2 can inhibit osteosarcoma invasion and migration as well as decrease osteosarcoma colony formation and proliferation [46]. As one of the few heart-specific splicing factors, previous studies of RBM20, which belongs to the same class, have mostly concentrated on research in cardiomyopathy. Specific genes involved in sarcomere assembly, ion transport, and relaxation function have been shown to be regulated by RBM20. It acts on actin and tropomyosin in familial cardiomyopathy, affecting striated muscle biomechanics. In addition, RBM20 has been implicated in fasting blood glucose regulation of insulin damage in cardiac tissue [47]. However, the role of RBM20 in osteosarcoma has not been proven so far. WIFE3 is also rarely reported in osteosarcoma and is currently only reported in a few cancers such as gastric cancer and breast cancer. *Cava et al.* [48] argued that with the increased aggressiveness of breast cancer molecular subtypes, the interaction between DERBPs and DEGs is one of the essential factors for the future progress of breast cancer research. By analyzing the microarray data of gastric cancer tissue, suggesting that the abnormal expression of WIFE3 is connected to the survival rate of patients with gastric cancer, *Zhou et al.* [49] discovered four RBPs (RBPMS2, DAZ1, WIFE3, and NOVA1) which independently predicted the prognosis of gastric cancer. However, DAZ1 and WIFE3 have not yet been reported in osteosarcoma, which indicates that they might be potential therapeutic targets and prognostic indicators for osteosarcoma. We found that alternative splicing events regulated by WIFE3-BSCL2 were positively associated with plasma cells in metastatic osteosarcoma tissue. Nonetheless, it remains unclear how WIFE3 affects splicing complex formation and pre-mRNA structure after binding to target gene sequences. In the future, we plan to conduct a more in-depth study on the specific molecular mechanism of WIFE3 regulating the alternative splicing of target genes.

Conclusion

We identified a total of 547 differentially alternative splicing events in metastatic osteosarcoma tissues, screened the top 7 DERBPs and associated alternative splicing events with different types of immune cells. Finally, analyzed their co-expression relationships. Among them, the alternative splicing event ZNF410 regulated by CYRAB has negatively correlated with T cells CD4 memory activated, and the alternative splicing event BSCL2 regulated by WIFE3 was positively correlated with plasma cells. In conclusion, we speculate that CYRAB and WIFE3 may affect the composition of immune cells by regulating gene alternative splicing, thereby promoting the metastasis of osteosarcoma tissue. Does ZNF410 or WIFE3 affect the formation of splicing complexes after binding to target genes to regulate the alternative splicing process? And the specific molecular mechanism of ZNF410 or

WIPF3 regulating target gene alternative splicing needs further study.

Declarations

Conflicts of interest: The authors declare that the research was conducted in the absence of any commercial or financial relationships that could be construed as a potential conflict of interest.

Data availability statement: Publicly available datasets were analyzed in this study. This data can be found here: The data for this study can be found in the GEO database (<https://www.ncbi.nlm.nih.gov/geo/query/acc.cgi?acc=GSE87624>).

Funding Statement: The National Natural Science Foundation of China (81401790).

References

1. Leichter AL, Sullivan MJ, Eccles MR, Chatterjee A. MicroRNA expression patterns and signalling pathways in the development and progression of childhood solid tumours. *Mol Cancer*. 2017; 16: 15.
2. Chen C, Xie L, Ren T, Huang Y, Xu J, et al. Immunotherapy for osteosarcoma: Fundamental mechanism, rationale, and recent breakthroughs. *Cancer Lett*. 2021; 500: 1-10.
3. Lv T, Jian Z, Li D, Ao R, Zhang X, et al. Oxyresveratrol induces apoptosis and inhibits cell viability via inhibition of the STAT3 signaling pathway in Saos-2 cells. *Mol Med Rep*. 2020; 22: 5191-5198.
4. Liao S, Zhou S, Wang C. GAPLINC is a predictor of poor prognosis and regulates cell migration and invasion in osteosarcoma. *Biosci Rep*. 2018; 38.
5. Czarnecka AM, Synoradzki K, Firlej W, Bartnik E, Sobczuk P, et al. Molecular Biology of Osteosarcoma. *Cancers (Basel)*. 2020; 12.
6. Ho XD, Phung P, V Q. Le, V H. Nguyen, Reimann E, Prans E, Köks G, et al. Whole transcriptome analysis identifies differentially regulated networks between osteosarcoma and normal bone samples. *Exp Biol Med (Maywood)*. 2017; 242: 1802-1811.
7. Castello A, Fischer B, Eichelbaum K. Insights into RNA biology from an atlas of mammalian mRNA-binding proteins. *Cell*. 2012; 149: 1393-1406.
8. Castello A, Fischer B, Frese Ck. Comprehensive Identification of RNA-Binding Domains in Human Cells. *Mol Cell*. 2016; 63: 696-710.
9. Gerstberger S, Hafner M, Tuschl T. A census of human RNA-binding proteins. *Nat Rev Genet*. 2014; 15: 829-845.
10. Hentze M W, Castello A, Schwarzl T. A brave new world of RNA-binding proteins. *Nat Rev Mol Cell Biol*. 2018; 19: 327-341.
11. Kim D, Pertea G, Trapnell C. TopHat2: accurate alignment of transcriptomes in the presence of insertions, deletions and gene fusions. *Genome Biol*. 2013; 14: R36.
12. Jin L, Li G, Yu D. Transcriptome analysis reveals the complexity of alternative splicing regulation in the fungus *Verticillium dahliae*. *BMC Genomics*. 2017; 18: 130.
13. Xia H, Chen D, Wu Q. CELF1 preferentially binds to exon-intron boundary and regulates alternative splicing in HeLa cells. *Biochim Biophys Acta Gene Regul Mech*. 2017; 1860: 911-921.
14. Xie C, Mao X, Huang J. KOBAS 2.0: a web server for annotation and identification of enriched pathways and diseases. *Nucleic Acids Res*. 2011; 39: W316-W322.
15. Yang B, Su Z, Chen G. Identification of prognostic biomarkers associated with metastasis and immune infiltration in osteosarcoma. *Oncol Lett*. 2021; 21: 180.
16. Chen T, Zhao L. Patrolling monocytes inhibit osteosarcoma metastasis to the lung. *Aging (Albany NY)*. 2020; 12: 23004-23016.
17. Montalbano M, Mcallen S, Sengupta U. Tau oligomers mediate aggregation of RNA-binding proteins Musashi1 and Musashi2 inducing Lamin alteration. *Aging Cell*. 2019; 18: e13035.
18. Glisovic T, Bachorik J L, Yong J. RNA-binding proteins and post-transcriptional gene regulation. *FEBS Lett*. 2008; 582: 1977-1986.
19. Coomer A O, Black F, Greystoke A. Alternative splicing in lung cancer. *Biochim Biophys Acta Gene Regul Mech*. 2019; 186: 194388.
20. Li B, Fang L, Wang B. Identification of Prognostic RBPs in Osteosarcoma. *Technol Cancer Res Treat*. 2021; 20: 2091220490.
21. Hu R, Zhu X, Chen C. RNA-binding protein PUM2 suppresses osteosarcoma progression via partly and competitively binding to STAR13 3'UTR with miRNAs. *Cell Prolif*. 2018; 51: e12508.
22. Wang L, Aireti A, Aihaiti A. Expression of microRNA-150 and its Target Gene IGF2BP1 in Human Osteosarcoma and their Clinical Implications. *Pathol Oncol Res*, 2019; 25: 527-533.
23. Pan W, Pang J, Ji B. RNA binding protein HuR promotes osteosarcoma cell progression via suppressing the miR-142-3p/HMGA1 axis. *Oncol Lett*. 2018; 16: 1475-1482.
24. Cheng C, Ding Q, Zhang Z. PTBP1 modulates osteosarcoma chemoresistance to cisplatin by regulating the expression of the copper transporter SLC31A1. *J Cell Mol Med*. 2020; 24: 5274-5289.
25. Niu J, Zhao X, Liu Q. Knockdown of MSI1 inhibited the cell proliferation of human osteosarcoma cells by targeting p21 and p27. *Oncol Lett*. 2017; 14: 5271-5278.
26. Cao Y, Di X, Zhang Q. RBM10 Regulates Tumor Apoptosis, Proliferation, and Metastasis. *Front Oncol*. 2021; 11: 603932.
27. Rothzerg E, Ho X D, Xu J. Alternative splicing of leptin receptor overlapping transcript in osteosarcoma. *Exp Biol Med (Maywood)*. 2020; 245: 1437-1443.
28. Jia R, Li C, Mccoy Jp. SRP20 is a proto-oncogene critical for cell proliferation and tumor induction and maintenance. *Int J Biol Sci*. 2010; 6: 806-826.
29. Ajiro M, Jia R, Yang Y. A genome landscape of SRSF3-regulated splicing events and gene expression in human osteosarcoma U2OS cells[J]. *Nucleic Acids Res*. 2016; 44: 1854-1870.
30. Fujiwara-Akita H, Maesawa C, Honda T. Expression of human telomerase reverse transcriptase splice variants is well correlated with low telomerase activity in osteosarcoma cell lines. *Int J Oncol*. 2005; 26: 1009-1016.
31. Shibutani M, Maeda K, Nagahara H. Tumor-infiltrating Lymphocytes Predict the Chemotherapeutic Outcomes in Patients with Stage IV Colorectal Cancer. *In Vivo*. 2018; 32: 151-158.
32. De PALMA M, LEWIS C E. Macrophage regulation of tumor responses to anticancer therapies. *Cancer Cell*. 2013; 23: 277-286.

33. Mantovani A, Marchesi F, Malesci A. Tumour-associated macrophages as treatment targets in oncology. *Nat Rev Clin Oncol*. 2017; 14: 399-416.
34. Kelleher F C, O'sullivan H. Monocytes, Macrophages, and Osteoclasts in Osteosarcoma. *J Adolesc Young Adult Oncol*. 2017; 6: 396-405.
35. Rosenberg J, Huang J. CD8(+) T Cells and NK Cells: Parallel and Complementary Soldiers of Immunotherapy. *Curr Opin Chem Eng*. 2018; 19: 9-20.
36. Sica A, Larghi P, Mancino A. Macrophage polarization in tumour progression. *Semin Cancer Biol*. 2008; 18: 349-355.
37. Saito T, Nishikawa H, Wada H. Two FOXP3(+) CD4(+) T cell subpopulations distinctly control the prognosis of colorectal cancers. *Nat Med*. 2016; 22: 679-684.
38. Gao K, Li X, Zhang L. Transgenic expression of IL-33 activates CD8(+) T cells and NK cells and inhibits tumor growth and metastasis in mice[J]. *Cancer Lett*. 2013; 335: 463-471.
39. Zhang Y L, Li Q, Yang XM. SPON2 Promotes M1-like Macrophage Recruitment and Inhibits Hepatocellular Carcinoma Metastasis by Distinct Integrin-Rho GTPase-Hippo Pathways. *Cancer Res*. 2018; 78: 2305-2317.
40. Zhao L, Zhang J, Liu Z. Comprehensive Characterization of Alternative mRNA Splicing Events in Glioblastoma: Implications for Prognosis, Molecular Subtypes, and Immune Microenvironment Remodeling. *Front Oncol*. 2020; 10: 555632.
41. Cuello MA, Kato S, Liberona F. The impact on high-grade serous ovarian cancer of obesity and lipid metabolism-related gene expression patterns: the underestimated driving force affecting prognosis. *J Cell Mol Med*. 2018; 22: 1805-1815.
42. Hossain M A, Saiful I S, Quinn J. Machine learning and bioinformatics models to identify gene expression patterns of ovarian cancer associated with disease progression and mortality. *J Biomed Inform*. 2019; 100: 103313.
43. Benanti J A, Williams D K, Robinson K L. Induction of extracellular matrix-remodeling genes by the senescence-associated protein APA-1. *Mol Cell Biol*. 2002; 22: 7385-7397.
44. Li X, Zhu J, Qiu J. Identification of Potential Prognostic Biomarkers for Breast Cancer Based on lncRNA-TF-Associated ceRNA Network and Functional Module. *Biomed Res Int*. 2020; 2020: 5257896.
45. Zhou H, Hu Y, Luo R. Multi-region exome sequencing reveals the intratumoral heterogeneity of surgically resected small cell lung cancer. *Nat Commun*. 2021; 12: 5431.
46. Cao Y, Di X, Zhang Q. RBM10 Regulates Tumor Apoptosis, Proliferation, and Metastasis. *Front Oncol*. 2021; 11: 603932.
47. Guo W, Schafer S, Greaser ML. RBM20, a gene for hereditary cardiomyopathy, regulates titin splicing. *Nat Med*. 2012; 18: 766-773.
48. Cava C, Armaos A, Lang B. Identification of long non-coding RNAs and RNA binding proteins in breast cancer subtypes. *Sci Rep*. 2022; 12: 693.
49. Zhou L, Zhou Q, Wu Y. Integrating 13 Microarrays to Construct a 6 RNA-binding proteins Prognostic Signature for Gastric Cancer patients. *J Cancer*. 2021; 12: 4971-4984.